Carbohydrate Polymers 116 (2015) 2–8

Contents lists available at ScienceDirect

Carbohydrate Polymers

journal homepage: www.elsevier.com/locate/carbpol

New supramolecular metallo-terpyridine carboxymethyl cellulose derivatives with antimicrobial properties

Enas A. Hassan[a], Mohammad L. Hassan[a,b,*], Charles N. Moorefield[c], George R. Newkome[c,d]

[a] Cellulose and Paper Department, National Research Centre, Dokki, Giza 12622, Egypt
[b] Centre of Excellence for Advanced Sciences, Advanced Materials and Nanotechnology Group, National Research Centre, Dokki, Giza 12622, Egypt
[c] Department of Polymer Science, The University of Akron, Akron, OH 44325, USA
[d] Department of Chemistry, The University of Akron, Akron, OH 44325, USA

ARTICLE INFO

Article history:
Received 31 December 2013
Received in revised form 17 June 2014
Accepted 18 June 2014
Available online 1 July 2014

Keywords:
Carboxymethyl cellulose
Terpyridine
Supramolecular
Antimicrobial

ABSTRACT

Preparation of a new water-soluble, cellulose derivative *via* a supramolecular route is presented. In a one-step procedure, carboxymethyl cellulose (CMC) was reacted with the $Cu(BF_4)_2$ complex of 4′-chloro[2,2′:6′,2″]terpyridine to generate the desired CMC–Cu^{II}–terpyridine derivative. This polymeric salt was characterized by elemental analysis, ultraviolet–visible spectroscopy (UV–visible), Fourier transform infrared (FTIR), X-ray diffraction (XRD), X-ray photoelectron spectroscopy (XPS), rheological properties measurements, thermogravimetric analysis (TGA), dynamic mechanical thermal analysis (DMTA), and tensile strength properties testing. In addition, antimicrobial properties were demonstrated against Gram-positive bacteria (*Staphylococcus aureus* and *Streptococcus thermophilus*), Gram-negative bacteria (*Escherichia coli*), and yeast (*Saccharomyces cervisiae*). The minimum inhibitory concentration of the prepared metallo-terpyridine CMC derivative against the studied microorganisms ranged from 6 to 8 mg/L to achieve ≥90% of microbial growth inhibition.

1. Introduction

The practice of using cellulose for preparation of new polymeric derivatives has been on-going for more than a century. Carboxymethyl cellulose (CMC, **1**) is an important as well as very useful carboxylate-modified, ether derivative, consisting of two units: β-D-glucose and β-D-glucopyranose 2-*O*-(carboxymethyl) monosodium salts, which are connected *via* β-1,4-glycosidic bonds. Attachment of the carboxymethyl moieties occurs predominantly at the C-2 and C-6 glucose positions with a preference for C-6 *vs.* C-2 (Heinze & Pfeiffer, 1999). Its water solubility, rheological properties, non-toxicity, and polyelectrolyte nature favor its use in many diverse applications, such as food additives (Parvar, Tehrani, Razavi, & Koocheki, 2013), pharmaceutics (Chukwumezie, Wojcik, Malak, & Adeyeye, 2002), bone regeneration (Jiang, Li, Zhang, & Wang, 2009), adhesives (Kawamoto, 2003), textiles (Krizova & Wiener, 2013), pesticides (Nisar, Kumar, Shakil, Pankaj, & Parmar, 2009), detergents (Verraest, Peters, van Bekkum, & van Rosmalen, 1996), paper (Li, Liu, Xu, & Xu, 2010; Watanabe, Gondo, & Kitao, 2004), and ceramic binders (Khosrowshahi & Salem, 2011).

In spite of the numerous desirable properties of CMC, it still lacks resistance to microbial attack due to its polysaccharide nature and absence of antimicrobial functional groups. Different routes have been studied to impart CMC antimicrobial properties, such as: the addition of antimicrobial agents (Liu, Han, Zhang, Li, & Li, 2012; Ng & Jumaat, 2014; Sayanjali, Ghanbarzadeh, & Ghiassifar, 2011); metal nanoparticles (Hebeish, Hashem, El-Hady, & Sharaf, 2013; Malmiri, Tan, Rahman, & Osman, 2013; Percival et al., 2012; Valappil et al., 2013; Zhong, Oporto, Jaczynski, Tesfai, & Armstrong, 2013), antimicrobial polymers (Yu et al., 2013); and grafting with other moieties possessing antimicrobial activity (El-Sherbiny, Salama, & Sarhan, 2009).

Terpyridines are *N*-heterocycles that exhibit high binding affinity toward transition metal ions due to strong dπ–pπ* back-bonding of the metal to the pyridine rings and the chelate effect. These terpyridine metal complexes possess distinct photophysical, electrochemical, and magnetic properties and have been widely investigated (Schubert, Winter, & Newkome, 2011). Notably, antimicrobial properties of terpyridine metal complexes have been investigated (El Basel Hassanien, 2004; Kharadi, 2014;

* Corresponding author at: Cellulose and Paper Department, National Research Centre, Dokki, Giza 12622, Egypt. Tel.: +1 202 33335926; fax: +1 202 33370931.
E-mail addresses: mlhassan2012@yahoo.com, mlhassan2013@yahoo.com (M.L. Hassan).

http://dx.doi.org/10.1016/j.carbpol.2014.06.056
0144-8617/

Kharat, Foroutannejad, & Khavasi, 2012; Naseri, Kharat, Banavand, Bakhoda, & Foroutannejad, 2012; Pandrala et al., 2013; Patel, Singh, Shukla, Gundla, & Chauhan, 2006; Patel, Parmar, Gandhi, & Thakkar, 2010; Patel, Joshi, & Patel, 2012a; Patel, Dosi, & Bhatt, 2012).

Terpyridine-containing polymers have also been investigated in which terpyridine ligands have been (1) incorporated into monomers that were subsequently polymerized, (2) attached as polymeric chain ends to be utilized in the formation of block copolymers, and (3) attached to polymeric backbone to generate new materials utilizing the available pendent terpyridine units that can be further transformed into metallo-supramolecular assemblies (Aamer & Tew, 2007; Breul et al., 2013; Chiper, Hoogenboom, & Schubert, 2009, 2010; Constable, 2007; Dobrawa, Ballester, Saha-Möller, & Würthner, 2006; Hassan, Moorefield, Elbatal, & Newkome, 2012; Hassan, Moorefield, Elbatal, & Newkome, et al., 2012; Köytepe, Demirel, & Seçkin, 2013; Köytepe, Demirel, Gültek, & Seçkin, 2013; Li, Guo, et al., 2013; Li, Zhu, et al., 2013; Maeda, Sakamoto, & Nishihara, 2013; Muronoi, Zhang, Higuchi, & Maki, 2013; Yang et al., 2013; Zhang, Zhang, & Chen, 2006); however, to the best of our knowledge, none of the terpyridine-containing metallopolymers have been investigated regarding their antimicrobial properties.

We have recently reported the preparation of terpyridine-modified cellulose nanocrystals *via* etherification of cellulose with 4′-chloro[2,2′:6′,2″]terpyridine (Cltpy) and subsequently examined their ability to assemble to metallo-supramolecular cellulose derivatives (Hassan, Moorefield, Elbatal, & Newkome, 2012; Hassan, Moorefield, Elbatal, & Newkome, et al., 2012). Herein, we report the preparation of water-soluble, terpyridine-based, supramolecular cellulose composite and demonstrate its utilitarian antimicrobial activity.

2. Experimental

2.1. Materials

Carboxymethyl cellulose (CMC) was obtained as a high viscosity grade (1000–1500 mPa for 4% in water at 25 °C) with DS of 0.93 as determined by the standard method (ASTM, 1961). 4′-Chloro[2,2′:6′,2″]terpyridine (Cltpy; assay 99%), $Cu(BF_4)_2{\cdot}6H_2O$ (assay 99%), NaOH, and absolute EtOH were obtained from Sigma-Aldrich and used, as received.

2.2. Preparation of CMC–Cu^{II}–terpyridine

The 4-Cl-terpyridine–$Cu(BF_4)_2$ [Cltpy–$Cu(BF_4)_2$] adduct was synthesized according to a previously published procedure (Wang et al., 2006). Reaction of Cltpy–$Cu(BF_4)_2$ (1.5 g, 6.82 mmol) with an aqueous solution of CMC (1 g in 150 mL of water) at 70 °C for 3 h generated the desired CMC–Cu^{II}tpyCl(BF_4) (**I**) along with a minor insoluble, cross-linked CMC–Cu^{II}–tpyCl (**II**), which was easily filtered. The filtrate contains the desired soluble CMC–Cu^{II}terpyCl(BF_4) (**I**) (Scheme 1), which was collected and purified by repeated precipitation and finally washing from/with an EtOH/water (7:3) mixture.

2.2.1. Characterization of CMC–Cu^{II}tpyCl(BF_4)

UV–visible spectra were recorded on UV-2450 Shimadzu spectrophotometer. The X-ray diffraction patterns were recorded using. The wave length of the Cu/$K\alpha$ radiation source was 0.154 nm and the spectra were obtained at a 30 mA with an accelerating voltage of 40 kV. A Perkin-Elmer Thermogravimetric analyzer was used to study thermal stability. The heating rate was set at 10 °C/min over a temperature range of 50–800 °C. Measurements were conducted under N_2 with a flow rate of 50 cm^3/min. XPS studies were performed using a Thermo Scientific K-ALPHA, XPS, England. Infrared spectra were obtained by using JASCO FTIR 800 E spectrometer. The samples were measured using the KBr disc technique. The elemental analysis was conducted on a Vario EI Elementar instrument. Degree-of-substitution (DS) of cellulose derivative was calculated from the nitrogen content as follows:

$$DS_x = \frac{M_c \times \%X}{100 \times M_x - \Delta M \times \%X}$$

where M_c is the molar mass of CMC monomeric unit at DS = 1; $\%X$ is the element or group; M_x is the molar mass of the element or the group; $\Delta M = M_s - M_L$, where, M_s is the molar mass of the substituent; M_L is the molar mass of the leaving group; and ΔM is the increase in molar mass of the monomeric unit at DS = 1.

Rheology of an aqueous solution (0.5 wt %) of CMC or CMC–Cu^{II}tpyCl(BF_4) (**I**) was studied using Anton Paar Rheometer (Anton Paar, Austria); a 2.5 cm plate and plate system was used at 25 ± 0.1 °C and a shear rate from 1 to 500 min^{-1}. Films were casted from aqueous solution (0.5 wt%) of CMC and **I**; each was dried in an oven under air circulation at 40 °C for 12 h. After drying, the films were conditioned at 50% relative humidity and 25 °C for 48 h before testing. Dynamic mechanical thermal properties of the films were measured using the same machine in tensile mode at a frequency of 1 Hz, strain of 0.1%, and at the heating rate of 3 °C/min over the temperature range of 25 to 200 °C. Tensile properties of the films were measured using a Lloyd universal testing machine (Lloyd, England) at crosshead speed of 2 mm/min using a load cell of 0.1 kN. The width of the films was 1 cm and the gauge length was 4 cm.

The antimicrobial activity of CMC and CMC–CltpyCu^{II}(BF_4) was evaluated by minimal inhibitory concentrations test (MIC). Gram-positive bacteria (*Staphylococcus aureus* and *Streptococcus thermophilus*), Gram-negative bacteria (*Escherichia coli*), as well as yeast (*Saccharomyces cervisiae*) were used, as test organisms. A pre-culture of bacteria and yeast was grown in Tryptic Soy Broth medium with 0.6% yeast extract overnight at 37 or 30 °C for bacteria and yeast, respectively. The inoculums were prepared by diluting an overnight culture grown in Tryptic Soy Broth. Each microorganism culture was exposed to different concentrations (1, 2, 4, 6, and 8 mg/mL) of the modified CMC–CltpyCu^{II}(BF_4) and incubated at 37 or 30 °C with shaking at 140 rpm. After a 24 h incubation, a series of solutions were prepared by addition of 1 mL of each culture to 9 mL of sterile 0.3 mM phosphate buffer (pH 6.8), followed by seeding 100 μL of each culture solution onto an agar plate. The plates were incubated at 37 or 30 °C, according to the type of microorganism for 24 h and the surviving cells counted. The antimicrobial activity was expressed as a reduction of the bacterial colonies after contact with the test specimen and compared to the number of bacterial colonies from the control. The percentage reduction (inhibition) was calculated using the following equation:

$$\text{reduction} = \frac{B - A}{B} \times 100$$

where, A are the surviving cells (CFU—colony forming units) for the plates containing the treated substrate and B are the surviving cells from the control.

3. Results and discussion

3.1. Preparation and characterization of CMC-CltpyCu^{II}(BF_4)

Reaction between CMC and $Cu(BF_4)_2$-tpyCl created a pentacoordinate complex involving the carboxylate groups of CMC (Wang et al., 2006); two main reactions occur leading to the formation of a complex between at least one carboxylic group of CMC chain and CMC-CltpyCu(BF_4) (Scheme 1; product **I**) or the complex between two carboxylic groups of two different CMC chains and

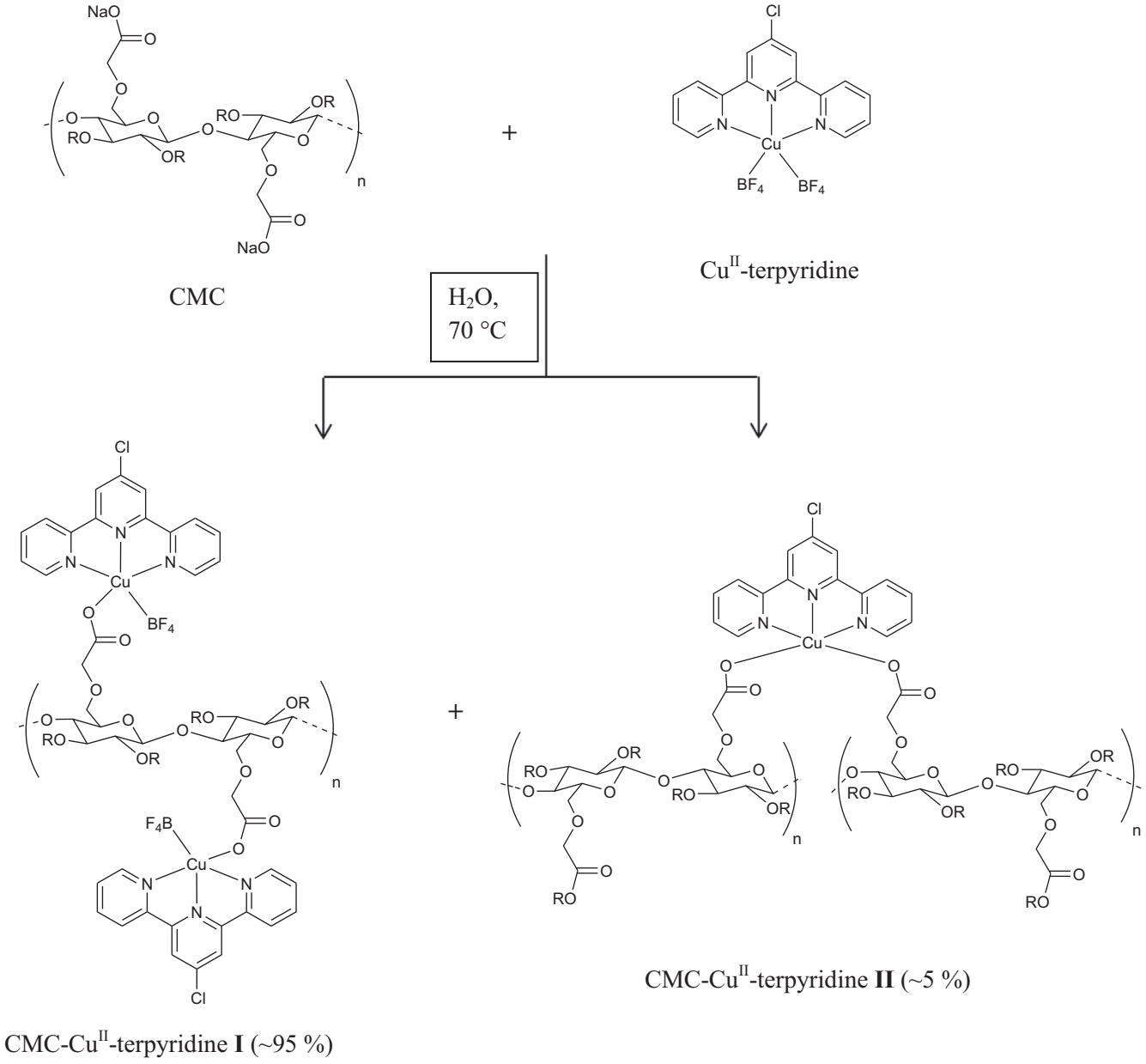

Scheme 1. Reaction between carboxymethyl cellulose (CMC) and Cu^{II}–terpyridine.

CMC–Cu–Cltpy (Scheme 1; product **II**). The second reaction needs a specific orientation of two CMC chains and $Cu(BF_4)_2$–Cltpy and leading to an increase in viscosity and the formation of a cross-linked product possessing low solubility. Taking into account the semi-rigid nature of CMC, formation of **II** is expected to be a minor component relative to **I**.

Thus, the major product **I** exhibited no notable increase in viscosity of the reaction mixture; whereas, traces (~5% by weight) of the cross-linked **II** that were obtained as an insoluble gel were easily removed by simple filtration. Nitrogen content of CMC–Cu^{II}Cltpy(BF_4) (**I**) was determined to be 2.18% indicating an *ca.* 0.77 degree-of-substitution (DS). The lower DS value of **I** than CMC suggests that not all of the CMC carboxylate groups form complexes with the $Cu(BF_4)_2$–tpyCl; notably, a reduced amount of Cu^{II}–tpyCl attachment at C-3 is expected due to steric hindrance. Fig. 1 shows the viscosity/shear rate curves for aqueous solutions (0.5 wt%) of CMC and CMC–CuCltpy(BF_4). The CMC exhibits its well-known, non-Newtonian pseudoplastic behavior with a viscosity decrease as the shear rate increases (Lindberg, Sirviö, & Martinmaa, 1987). The decrease in viscosity is attributed to the diminished CMC chain interaction and reduction of macromolecular aggregation, which is common for polysaccharide polyelectrolytes in aqueous solution (Almedia & Dias, 1997). At low shear rates, the viscosity significantly decreased; whereas at higher shear rates, the changes in viscosity were lower. The CMC also exhibited a higher viscosity than **I**, since attaching $Cu(BF_4)_2$–tpyCl to the carboxylate groups of the polysaccharide reduced the interactions between the chains. The lower viscosity of **I** relative to CMC supports its formation too

Further support for the formation of **I** was obtained by UV–visible spectroscopy, X–ray diffraction, and XPS. Fig. 2 shows UV–visible spectra of CMC, $Cu(BF_4)_2$–tpyCl, and CMC–CutpyCl(BF_4) (**I**). The $Cu(BF_4)_2$–tpyCl exhibited two main absorption bands at *ca.* 350 and 680 nm that are attributed to the conjugated aromatic rings (π–π^* absorption band associated with the terpyridine *N*-electrons) and metal-to-ligand-charge-transfer (MLCT) of the tridentate terpyridine–Cu^{II} unit (Fallahpour, 2003). A blue shift of the MLCT

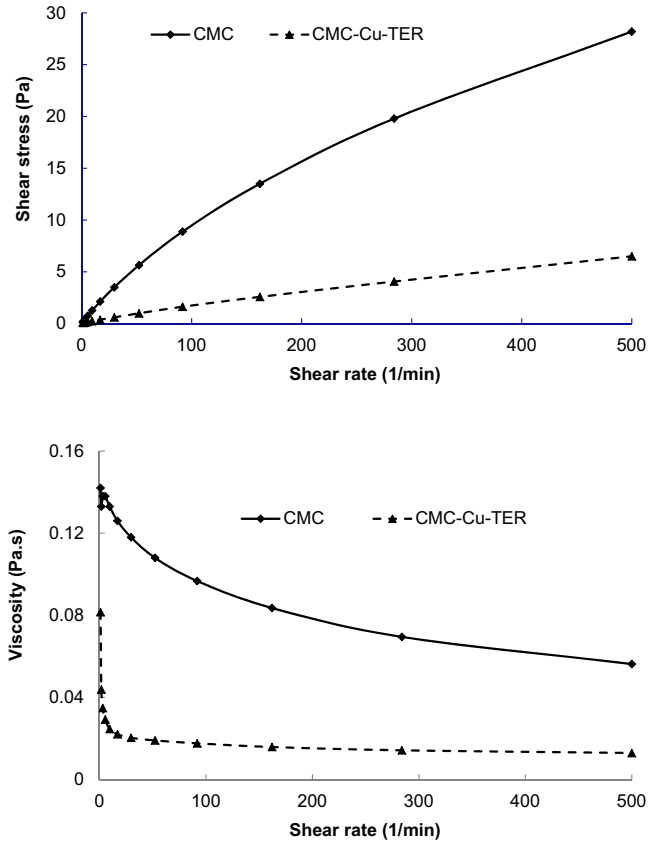

Fig. 1. Rheological properties of carboxymethyl cellulose (CMC) and CMC–Cu^{II}–terpyridine (CMC–Cu–TER).

absorption band from 680 to 660 nm was also observed upon terpyridine–Cu^{II}–carboxylate complexation.

Fig. 3 shows FTIR spectra of CMC, $Cu(BF_4)_2$–tpyCl, and **I**. The CMC showed its known broad bands at 3690–2990 cm^{-1} (O—H stretching), 2960–2855 cm^{-1} (C—H stretching), 1618 cm^{-1} (CO_2^- stretching), 1435 cm^{-1} (C—H scissoring for the CH_2 groups), 1300 cm^{-1} (O—H bending), and 1042 cm^{-1} (C—O—C stretching) (Rachtanapun, Luangkamin, Tanprasert, & Suriyatem, 2012). Whereas, $Cu(BF_4)_2$–tpyCl showed bands at 3694–3090 cm^{-1} (water O—H stretching), 3053 cm^{-1} (aromatic C—H stretching), 1415–1590 cm^{-1} (stretching vibration of aromatic ring), 1630 cm^{-1} (a shoulder for the C=N stretching), bands at 1034,

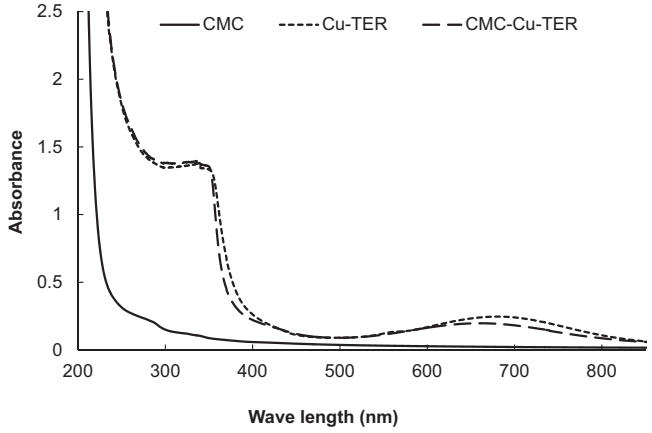

Fig. 2. UV–visible spectra of carboxymethyl cellulose (CMC), Cu^{II}–terpyridine (Cu–TER), and CMC–Cu^{II}–terpyridine (CMC–Cu–TER).

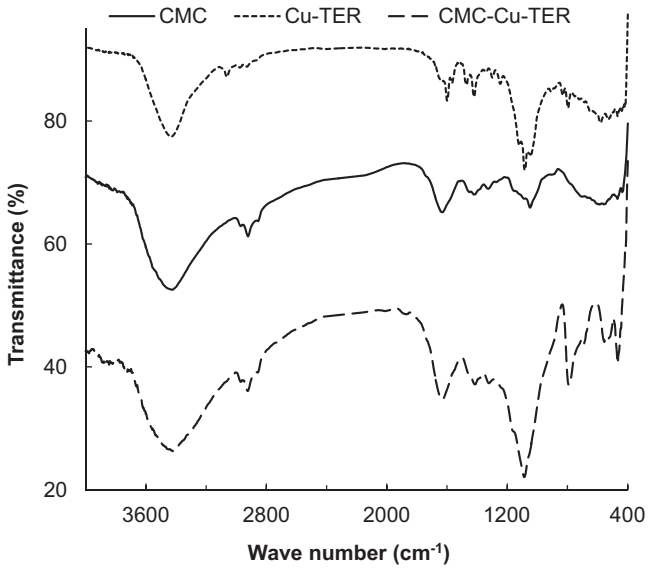

Fig. 3. FTIR spectra of carboxymethyl cellulose (CMC), Cu^{II}–terpyridine (Cu–TER), and CMC–Cu^{II}–terpyridine (CMC–Cu–TER).

1075, and 1108 cm^{-1} (BF_4), 796–890 cm^{-1} (substituted aromatic rings), weak bands at 635, 580, and 520 cm^{-1} (Cu—N and C—Cl stretching), respectively (Nakamoto, 1992; Fallahpour, 2003). As a result of complex formation to generate **I**, a new band of medium intensity appeared at ~ 470 cm^{-1} due to stretching vibration of Cu—O bond (Huang, You, Wang, & Yao, 2009) and the intensity of Cu—N peaks became stronger as well as shifted to 568 cm^{-1}. The medium intensity band at ~800 cm^{-1} in **I** was attributed coordination of water molecules to Cu metal ion (Nakamoto, 1992). Presence of BF_4^- broad band centered at 1100 cm^{-1} also supports the formation of CMC–CutpyCl(BF_4) (**I**).

XPS spectra (Fig. 4) showed the expected characteristic 2p Cu^{II} peaks with binding energies of 935.5 and 957 eV (Folmer & Jellinek, 1980) and slightly shifted peaks to 931.5 and 951.7 eV for both $Cu(BF_4)_2$–tpyCl and **I** species, respectively, providing further support for their structures.

Additional evidence supporting the formation of CMC–Cu^{II}tpyCl(BF_4) (**I**) can be observed in the differences in the XRD patterns of CMC and **I** (Fig. 5) in which the CMC showed a characteristic main peak at 2-theta values at *ca.* 21 (100% peak) (Mohkami & Talaeipour, 2011) with a d-spacing of 4.24 Å; whereas **I** exhibited a pattern possessing 2-theta peaks at 14, 16.9 (100% peak), 18.5, and 25.3 corresponding to *d*-spacing of 6.29, 5.28, 4.78, and 3.52 Å, respectively. The appearance of new peaks at 2-theta values of 16.9 (as the main peak) and at 13.6 as well as a change in d-spacing support the changes in the crystalline structure caused by attaching $Cu(BF_4)_2$–tpyCl onto CMC chains. Notably, $Cu(BF_4)_2$–tpyCl exhibits an XRD pattern possessing pertinent 2-theta peaks at 12.0, 18.2, 18.3 (100% peak), 25.6, corresponding to *d*-spacing of 7.32, 4.88, 4.86, and 3.49, respectively.

3.2. *Properties of CMC–Cu^{II}tpyCl(BF_4) film*

Since the CMC–CutpyCl(BF_4) (**I**) is water-soluble, it readily allows film casting from aqueous solution. Thermal stability, dynamic thermal mechanical, tensile strength, and anti-bacterial properties of films, prepared from CMC and **I** were studied. The TG curves (Fig. 6) of both films indicate initial weight loss from 50 to 150 °C due to loss of water. At *ca.* 240 °C, the CMC data reveal an onset thermal degradation and gas evolution (Bochek et al., 2012) resulting in a loss of *ca.* 48% of the weight. In comparison, the data

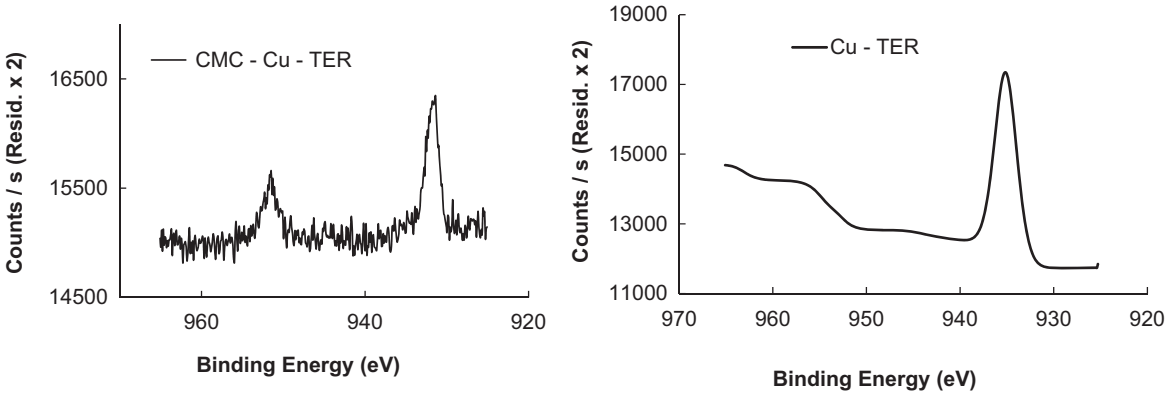

Fig. 4. XPS Copper 2*p* spectra of Cu^{II}–terpyridine (Cu–TER) and CMC–Cu^{II}–terpyridine (CMC–Cu–TER).

for **I** showed an onset degradation temperature at about 222 °C ending with a loss of weight 45%; whereas, the first derivative weight loss curves exhibited thermal degradation peaks at 286 °C (CMC) and 248 and 270 °C (**I**).

The DMTA plots (Fig. 7) of the films for CMC and **I** indicate changes in thermal properties of the non-modified polymer had occurred as a result of attaching Cutpycl(BF_4) units to its chain. The storage modulus of **I** was higher than that of CMC indicating higher stiffness of the film prepared from **I** than CMC due presumably to the presence of aromatic rings in the structure of Cu^{II}–tpyCl functionalized hybrid. The storage modulus curve of CMC began to decrease at *ca.* 210 °C, while **I** showed a beginning decrease at *ca.* 219 °C; whereas, the loss modulus curve was characterized by a broad peak at 129 °C attributed to the glass transition temperature and a peak at 230 °C assigned to localized crystalline melting of the polymer (Ghanbarzadeh & Almasi, 2011). In contrast, the loss modulus curve obtained for **I** showed peaks at about 125 and 250 °C corresponding to similar thermal transitions. The melting peak is above the onset degradation temperature of the polymer, as shown in the TGA curves. The higher temperature of the melting peak (250 °C) for **I** compared to that of the CMC indicates the presence of the bulky Cu(BF_4)$_2$–tpyCl moieties with their three connected aromatic rings and low mobility.

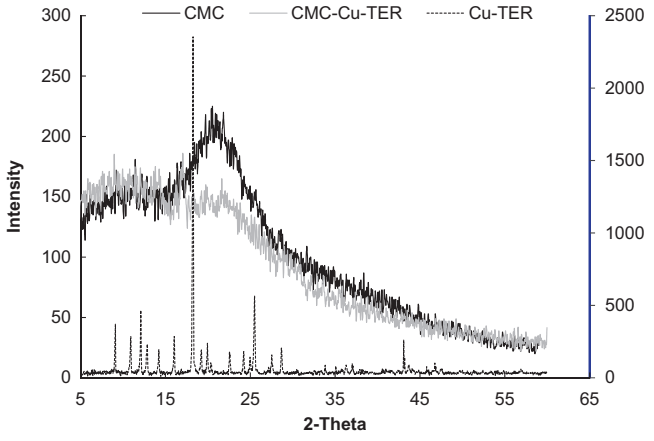

Fig. 5. XRD patterns of carboxymethyl cellulose (CMC), Cu^{II}–terpyridine (Cu–TER), and CMC–Cu^{II}–terpyridine (CMC–Cu–TER).

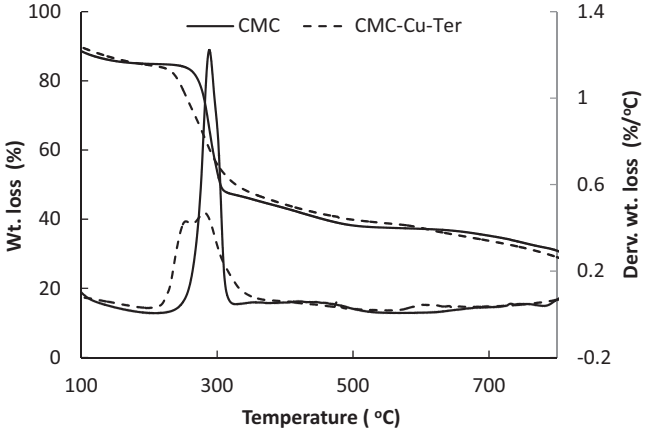

Fig. 6. TGA curves of carboxymethyl cellulose (CMC) and CMC–Cu^{II}–terpyridine (CMC–Cu–TER).

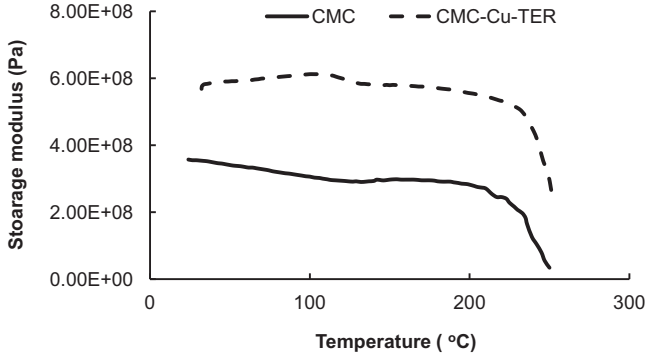

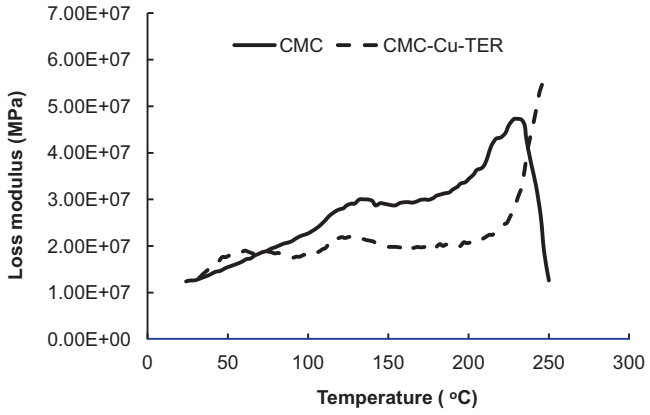

Fig. 7. DMTA curves of carboxymethyl cellulose (CMC) and CMC–Cu^{II}–terpyridine (CMC–Cu–TER).

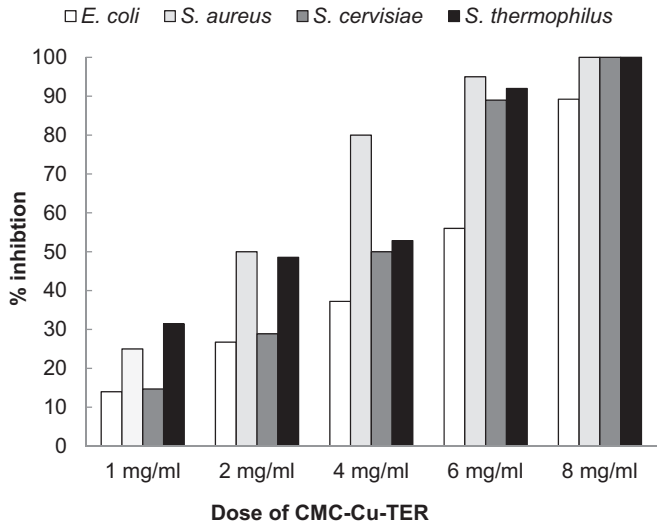

Fig. 8. Effect of CMC–Cu^{II}–terpyridine (CMC–Cu–TER) dose on growth inhibition of *Staphylococcus aureus*, *Streptococcus thermophilus*, *Escherichia coli*, and *Saccharomyces cervisiae*.

The film of **I** showed higher stiffness based on tensile strength when compared to the film from CMC. The increase in Young's modulus as a result of the introduction of $Cu(BF_4)_2$–tpyCl to CMC was about 46% while the tensile strength and elongation of film of **I** were lower than CMC by about 20 and 26%, respectively. The decrease in elongation-at-break is due to the higher stiffness within the film of **I**, while the decrease in tensile strength could be attributed to the reduced hydrogen-bonding between the carboxymethyl cellulose chains in their modified form.

3.3. Antimicrobial properties of CMC–CutpyCl(BF_4) films

The antimicrobial activity of CMC–CutpyCl(BF_4) was evaluated by minimal inhibitory concentrations test (MIC) using *S. aureus* and *S. thermophilus* (G +ve), *E. coli* (G −ve), and *S. cervisiae* yeast. The test can determine the minimum concentration of an antimicrobial material needed to inhibit growth of microorganisms. The grown inoculums containing the aforementioned microorganisms in Tryptic Soy Broth medium in the absence of cellulose derivatives was taken as the control sample.

Previous studies on terpyridine copper complexes showed antimicrobial properties of these complexes against some G +ve and G −ve bacteria (Li, Guo, et al., 2013; Naseri et al., 2012; Patel et al., 2010, 2012, 2012a). Copper complexes of terpyridines proved its ability to break DNA chains of bacteria. Chelation of Cu^{II} with ligands reduces polarity of metal ion by overlap of the ligand orbital and partial sharing of the positive charge of the metal ion with the donor groups. Increase in delocalization of π-electrons over the whole ligand enhances the penetration of complexes into lipid membranes and blocking of the metal binding sites in the enzymes of microorganisms (Chohan, Suparan, & Scozzafava, 2005). The complexes may also disturb the respiration process of the cell and thus blocking the synthesis of proteins, which restricts further growth of the organism and thus results in the overall gain in the biological potency (Patel et al., 2012).

In the current work, as shown in Fig. 8, **I** showed very good antimicrobial activity toward G +ve and G −ve bacteria as well as with the yeast studied. Decrease in number of colonies of bacteria and yeast was observed on increasing the concentration of **I**. At low concentration (1–2 mg/mL), **I** showed higher activity against the G +ve bacteria than G −ve and yeast studied. Complete inhibition of G +ve and yeast was obtained at 8 mg/mL dose of **I** while the inhibition was about 90% toward the G −ve *E. coli* at the same dose. The obtained results indicate that attaching $Cu(BF_4)_2$–tpyCl groups to CMC does not affect their known antimicrobial properties. The reason for the high MIC values than those usually reported for antimicrobial agents could be attributed to the polymeric nature of prepared cellulose derivative and the DS values of the CMC used and the prepared CMC-terpyridine derivative. However, such high values are not uncommon for antimicrobial cellulose modified derivatives (Jebali et al., 2013; Zhang et al., 2012).

4. Conclusions

New water–soluble cellulose derivatives were prepared *via* a supramolecular strategy by reaction of carboxymethyl cellulose with $Cu(BF_4)_2$–tpyCl complexes. The CMC–CutpyCl(BF_4) hybrid showed very good antimicrobial properties against Gram positive (*S. aureus* and *S. thermophilus)* and Gram negative bacteria (*E. coli*), as well as yeast (*S. cervisiae*). These types of cellulose polymers have potential applications as coating materials for functional paper products in packaging, medical textiles, as an additive for food products, and in pharmaceuticals. Cytotoxicity evaluations of these derivatives and utilitarian applications are ongoing.

Acknowledgment

The authors gratefully acknowledge the National Science Foundation, USA (GRN, CHE-11-51991) for financial support.

References

Aamer, K. A., & Tew, G. N. (2007). Supramolecular polymers containing terpyridine–metal complexes in the side chain. *Macromolecules*, *40*, 2737–2743.
Almedia, A. R., & Dias, M. L. (1997). Comparative study of shear degradation of carboxymethyl cellulose and poly(ethylene oxides) in aqueous solution. *Polymer Degradation and Stability*, *56*, 331–337.
ASTM. (1961). *Tentative methods of testing sodium carboxymethyl cellulose*. ASTM. D1439-61T.
Bochek, A. M., Shevchuk, I. L., Gavrilova, I. I., Nesterova, N. A., Panarin, E. F., Yudin, V. E., et al. (2012). Compatibility of carboxymethyl cellulose ionized to various degrees with poly-*N*-vinylformamide in composite films. *Russian Journal of Applied Chemistry*, *85*, 1413–1421.
Breul, A. M., Schäfer, J., Altuntas, E., Hager, M. D., Winter, A., Dietzek, B., et al. (2013). Incorporation of polymerizable osmium(II) bis-terpyridine complexes into PMMA backbones. *Journal of Inorganic and Organometallic Polymers and Materials*, *23*, 74–80.
Chiper, M., Hoogenboom, R., & Schubert, U. S. (2009). Toward main chain metallo-terpyridyl supramolecular polymers: The metal does the trick. *Macromolecular Rapid Communication*, *30*, 565–578.
Chiper, M., Hoogenboom, R., & Schubert, U. S. (2010). New terpyridine macroligands as potential synthons for supramolecular assemblies. *European Polymer Journal*, *46*, 260–269.
Chohan, Z. H., Suparan, C. T., & Scozzafava, A. (2005). Metal binding and antibacterial activity of ciprofloxacin complexes. *Journal of Enzyme Inhibition and Medicinal Chemistry*, *21*, 303–307.
Chukwumezie, B. N., Wojcik, M., Malak, P., & Adeyeye, M. C. (2002). Feasibility studies in spheronization and scale-up of ibuprofen microparticulates using the rotor disk fluid-bed technology. *AAPS PharmSciTech*, *3*, 10–22.
Constable, E. C. (2007). 2,2′:6′,2-Terpyridines: From chemical obscurity to common supramolecular motifs. *Chemical Society Reviews*, *36*, 246–253.
Dobrawa, R., Ballester, P., Saha-Möller, C. R., & Würthner, F. (2006). Thermodynamics of 2,2′:6′ 2-terpyridine–metal ion complexation. In U. S. Schubert, G. R. Newkome, & I. Manners (Eds.), *ACS Symposium Series 928 Metal-containing and metal-supramolecular polymers and materials (43-61)*. Washington, DC: American Chemical Society.
El Basel Hassanien, A. Z. A. (2004). 2,6-*Bis*[3-*N*,*N*-dimethylamino-1-oxopropen-1-yl]pyridine, as a building block in heterocyclic synthesis: Synthesis of [2,2′:6′,2]terpyridines and 2,6-*bis*[pyrazolyl, isoxazolyl, diazepinyl, pyrazolo[5,1-*a*]pyrimidinyl and pyrazolo[4,3-*d*]-pyridazinyl]pyridines. *Journal of Chemical Research*, *8*, 536–540.
El-Sherbiny, I. M., Salama, A., & Sarhan, A. A. (2009). Grafting study and antifungal activity of a carboxymethyl cellulose derivative. *International Journal of Polymeric Materials and Polymeric Biomaterials*, *58*, 453–467.
Fallahpour, R. A. (2003). Synthesis of 4′-substituted-2,2′:6′,2-terpyridines. *Synthesis*, *2*, 155–184.
Folmer, J. C. W., & Jellinek, F. (1980). The valence of copper in sulphides and selenides: An x-ray photoelectron spectroscopy study. *Less-Common Metals*, *76*, 153–162.

Ghanbarzadeh, B., & Almasi, H. (2011). Physical properties of edible emulsified films based on carboxymethyl cellulose and oleic acid. *International Journal of Biological Macromolecules*, *48*, 44–49.

Hassan, M. L., Moorefield, C. N., Elbatal, H. S., & Newkome, G. R. (2012). New metallo-supramolecular terpyridine modified cellulose functional nanomaterials. *Journal of Macromolecular Science Part A: Pure and Applied Chemistry*, *49*, 298–305.

Hassan, M. L., Moorefield, C. N., Elbatal, H. S., Newkome, G. R., Modarelli, D. A., & Romano, N. C. (2012). Fluorescent cellulose nanocrystals via supramolecular assembly of terpyridine-modified cellulose nanocrystals and terpyridine-modified perylene. *Materials Science and Engineering. Part B: Advanced Functional Solid Materials*, *177*, 350–358.

Hebeish, A., Hashem, M., El-Hady, M. M. A., & Sharaf, S. (2013). Development of CMC hydrogels loaded with silver nano-particles for medical applications. *Carbohydrate Polymers*, *92*, 407–413.

Heinze, T., & Pfeiffer, K. (1999). Studies on the synthesis and characterization of carboxymethyl cellulose. *Die Angewandte Makromolekulare Chemie*, *266*, 37–45.

Jebali, A., Hekmatimoghaddam, S., Behzadi, A., Rezapor, I., Mohammadi, B. H., Jasemizad, T., et al. (2013). Antimicrobial activity of nanocellulose conjugated with allicin and lysozyme. *Cellulose*, *20*, 2897–2907.

Malmiri, H. J., Tan, C. P., Rahman, R. A., & Osman, A. (2013). Developing a new antimicrobial edible coating formulation based on carboxymethyl cellulose-silver nanoparticles for tropical fruits and an in vitro evaluation of its antimicrobial properties. *ISHS Acta Horticulturae*, *1012*, 705–710.

Jiang, L., Li, Y., Zhang, L., & Wang, X. (2009). Preparation and characterization of a novel composite containing carboxymethyl cellulose used for bone repair. *Materials Science and Engineering C*, *29*, 193–198.

Kawamoto, T. (2003). Use of a new adhesive film for the preparation of multi-purpose fresh-frozen sections from hard tissues, whole-animals, insects and plants. *Archives of Histology and Cytology*, *66*, 123–143.

Kharadi, G. J. (2014). Effect of substituent of terpyridines on the *in vitro* antioxidant, antitubercular, biocidal and fluorescence studies of copper(II) complexes with clioquinol. *Spectrochimica Acta—Part A: Molecular and Biomolecular Spectroscopy*, *117*, 662–668.

Kharat, A. N., Foroutannejad, S., & Khavasi, H. R. (2012). Biological evaluation of 4′-(2-thienyl)[2,2′;6′,2]terpyridine-1,1-diium chloride tetrachloridoaurate(III): The effect of counter cations. *Synthesis and Reactivity in Inorganic Metal-Organic and Nano-Metal Chemistry*, *42*, 752–757.

Khosrowshahi, Y. B., & Salem, A. (2011). Influence of polyvinyl alcohol and carboxymethyl cellulose on the reliability of extruded ceramic body: Application of mixture design method in fabricating reliable ceramic raschig rings. *International Journal of Applied Ceramic Technology*, *8*, 1334–1343.

Köytepe, S., Demirel, M. H., & Seçkin, T. (2013). Synthesis and self-assembling properties of 2,2′:6′,2-terpyridine-based carbon nanotube coordination polymers. *Journal of Inorganic and Organometallic Polymers and Materials*, *23*, 1104–1112.

Köytepe, S., Demirel, M. H., Gültek, A., & Seçkin, T. (2013). Metallo-supramolecular materials based on terpyridine-functionalized polyhedral silsesquioxane. *Polymer International*, http://dx.doi.org/10.1002/pi.4596

Krizova, H., & Wiener, J. (2013). Development of carboxymethyl cellulose/polyphenols gels for textile applications. *Autex Research Journal*, *13*, 33–36.

Li, J., Liu, Q., Xu, L., & Xu, W. (2010). The application research of carboxymethyl cellulose in paper printing & packaging materials. In *Paper presented at the 17th IAPRI World Conference on Packaging 2010* (pp. 372–375).

Li, N., Guo, H.-L., Hu, H.-M., Song, J., Xu, B., Yang, M.-L., et al. (2013). Hydrothermal syntheses, crystal structures and luminescence properties of zinc(II) and cadmium(II) coordination polymers based on bifunctional [3,2′:6′,3]terpyridine-4′-carboxylic acid. *Journal of Solid State Chemistry*, *198*, 416–423.

Li, N., Zhu, Q.-E., Hu, H.-M., Guo, H.-L., Xie, J., Wang, F., et al. (2013). Hydrothermal syntheses, crystal structures and luminescence properties of zinc(II) coordination polymers constructed by bifunctional 4′-(4-carboxyphenyl)[3,2′:6′,3]terpyridine. *Polyhedron*, *49*, 207–215.

Lindberg, J. J., Sirviö, H., & Martinmaa, J. (1987). Rheological studies on CMC. *Cellulose Chemistry and Technology*, *21*, 379–385.

Liu, Q., Han, J., Zhang, Y., Li, S., & Li, J. (2012). Antimicrobial and antioxidant activities of carboxymethyl cellulose edible films incorporated with rosemary extracts on fresh beef during refrigerated storage. *Advanced Materials Research*, *554–556*, 1179–1184.

Huang, W., You, W., Wang, L., & Yao, C. (2009). Anionic effects on the formation of tridentate 4′-chloro-2,2′:6′,2-terpyridine copper(II) complexes having 1:1 or 1:2 ratio of metal and ligand and their crystal symmetry. *Inorganica Chimica Acta*, *362*, 2127–2135.

Maeda, H., Sakamoto, R., & Nishihara, H. (2013). Metal complex oligomer and polymer wires on electrodes: Tactical constructions and versatile functionalities. *Polymer*, *54*, 4383–4403.

Mohkami, M., & Talaeipour, M. (2011). Investigation of the chemical structure of carboxylated and carboxymethylated fibers from waste paper *via* XRD and FTIR analysis. *BioResources*, *6*, 1988–2003.

Muronoi, Y., Zhang, J., Higuchi, M., & Maki, H. (2013). Electrochemical switching of lumine-scence in Ru(II)-based metallosupramolecular polymer device. *Chemistry Letters*, *42*, 761–763.

Nakamoto, K. (1992). *Infrared and Raman spectra on inorganic and coordination complexes* (4th ed.). New York, NY: John Wiley and Sons.

Naseri, Z., Kharat, A. N., Banavand, A., Bakhoda, A., & Foroutannejad, S. (2012). First row transition metal complexes of thienyl substituted terpyridine: Structural, photophysical and biological studies. *Polyhedron*, *33*, 396–403.

Ng, S.-F., & Jumaat, N. (2014). Carboxymethyl cellulose wafers containing antimicrobials: A modern drug delivery system for wound infections. *European Journal of Pharmaceutical Sciences*, *51*, 173–179.

Nisar, K., Kumar, J., Shakil, N. A., Pankaj, W. S., & Parmar, B. S. (2009). Controlled release formulations of acephate: Water and soil release kinetics. *Journal of Environmental Science and Health—Part B, Pesticides, Food Contaminants and Agricultural Wastes*, *44*, 533–537.

Pandrala, M., Li, F., Feterl, M., Mulyana, Y., Warner, J. M., Wallace, L., et al. (2013). Chlorido-containing ruthenium(II) and iridium(III) complexes as anti-microbial agents. *Dalton Transactions*, *42*, 4686–4694.

Parvar, B. M., Tehrani, M. M., Razavi, S. M. A., & Koocheki, A. (2013). Application of simplex-centroid mixture design to optimize stabilizer combinations for ice cream manufacture. *Journal of Food Science and Technology*, http://dx.doi.org/10.1007/s13197-013-1133-5

Patel, M. N., Dosi, P. A., & Bhatt, B. S. (2012). Synthesis, characterization, antibacterial activity and DNA interaction studies of drug-based mixed ligand copper(II) complexes with terpyridines. *Medicinal Chemistry Research*, *21*, 2723–2733.

Patel, M. N., Joshi, H. N., & Patel, C. R. (2012). DNA interaction, in vitro antimicrobial and SOD-like activity of copper(II) complexes with norfloxacin and terpyridines. *Journal of Organometallic Chemistry*, *701*, 8–16.

Patel, M. N., Parmar, P. A., Gandhi, D. S., & Thakkar, V. R. (2010). Antimicrobial and nuclease activity of mixed polypyridylruthenium(II) complexes. *Inorganic Chemistry Communications*, *13*, 1480–1484.

Patel, R. N., Singh, N., Shukla, K. K., Gundla, V. L. N., & Chauhan, U. K. (2006). Synthesis, characterization and biological activity of ternary copper(II) complexes containing polypyridyl ligands. *Spectrochimica Acta—Part A: Molecular and Biomolecular Spectroscopy*, *63*, 21–26.

Percival, S. L., Thomas, J., Linton, S., Okel, T., Corum, L., & Slone, W. (2012). The antimicrobial efficacy of silver on antibiotic-resistant bacteria isolated from burn wounds. *International Wound Journal*, *9*, 488–493.

Rachtanapun, P., Luangkamin, S., Tanprasert, K., & Suriyatem, R. (2012). Carboxymethyl cellulose film from durian rind. *LWT—Food Science and Technology*, *48*, 52–58.

Sayanjali, S., Ghanbarzadeh, B., & Ghiassifar, S. (2011). Evaluation of antimicrobial and physical properties of edible film based on carboxymethyl cellulose containing potassium sorbate on some mycotoxigenic *Aspergillus* species in fresh pistachios. *LWT—Food Science and Technology*, *44*, 1133–1138.

Schubert, U. S., Winter, A., & Newkome, G. R. (2011). *Terpyridine-based materials for catalytic optoelectronic and life science applications*. Weinheim: Wiley-VCH.

Valappil, S. P., Yiu, H. H. P., Bouffier, L., Hope, C. K., Evans, G., Claridge, J. B., et al. (2013). Effect of novel antibacterial gallium-carboxymethyl cellulose on *Pseudomonas aeruginosa*. *Dalton Transactions*, *42*, 1778–1786.

Verraest, D. L., Peters, J. A., van Bekkum, H., & van Rosmalen, G. M. (1996). Carboxymethyl inulin: A new inhibitor for calcium carbonate precipitation. *Journal of the American Oil Chemists' Society*, *73*, 55–62.

Wang, P., Moorefield, C. N., Li, S., Hwang, S.-H., Shreiner, C. D., & Newkome, G. R. (2006). Terpyridine Cu^{II}-mediated reversible nanocomposites of single-wall carbon nanotubes: Towards metallo-nanoscale architectures. *Chemical Communication*, 1091–1093.

Watanabe, M., Gondo, T., & Kitao, O. (2004). Advanced wet-end system with carboxymethyl-cellulose. *Tappi Journal*, *3*, 15–19.

Yang, P., Wu, H., Lee, C., Chen, W., He, H., & Chen, M. (2013). Triphenylamine-based linear conjugated polyfluorenes with various pendant groups: Synthesis, characterization and ion responsive properties. *Polymer*, *54*, 1080–1090.

Yu, S.-H., Hsieh, H.-Y., Pang, J.-C., Tang, D.-W., Shih, C.-M., Tsai, M.-L., et al. (2013). Active films from water-soluble chitosan/cellulose composites incorporating releasable caffeic acid for inhibition of lipid oxidation in fish oil emulsions. *Food Hydrocolloids*, *32*, 9–19.

Zhang, D., Xie, J., Yu, P., Huang, X., Yang, M., & Liu, H. (2012). Antifungal activity and humidity sensitivity of quaternized cellulose synthesized in NaOH/urea aqueous solution. *Cellulose*, *19*, 189–198.

Zhang, L., Zhang, Y., & Chen, Y. (2006). Synthesis of bis[2,2′:6′,2-terpyridine]-terminated telechelic polymers by RAFT polymerization and ruthenium–polymer complexation thereof. *European Polymer Journal*, *42*, 2398–2406.

Zhong, T., Oporto, G. S., Jaczynski, J., Tesfai, A. T., & Armstrong, J. (2013). Antimicrobial properties of the hybrid copper nanoparticles-carboxymethyl cellulose. *Wood and Fiber Science*, *45*, 215–222.